JOHNSON MATTHEY
TECHNOLOGY REVIEW
www.technology.matthey.com

Johnson Matthey Highlights

A selection of recent publications by Johnson Matthey R&D staff and collaborators

Toward Reversible and Moisture-Tolerant Aprotic Lithium-Air Batteries

I. Temprano, T. Liu, E. Petrucco, J. H. J. Ellison, G. Kim, E. Jónsson and C. P. Grey, *Joule*, 2020, **4**, (11), 2501

In this study, reversable LiOH-based lithium-oxygen battery cycling was exhibited after introducing an ionic liquid to a DME-based electrolyte containing water and lithium iodide. The battery cycling operated with a low charging overpotential *via* a four-electron oxygen reduction process. By incorporating the ionic liquid, the redox potential of the I^-/I_3^- couple increased and therefore the charging mechanism switched from IO^-/IO_3^- formation to OER.

Lithium Ion Sites and their Contribution to the Ionic Conductivity of RLi_2O-B_2O_3 Glasses with $R \leq 1.85$

A. Ruckman, G. Beckler, W. Guthrie, M. Jesuit, M. Boyd, I. Slagle, R. Wilson, N. Barrow, N. S. Tagiara, E. I. Kamitsos, S. Feller and C. B. Bragatto, *Solid State Ionics*, 2021, **359**, 115530

A fast quenching technique was used to prepare high content lithium oxide glasses with no evidence of phase separation (up to $R = 1.85$). The glasses were employed to test the relationship between the number of loose lithium ions and the ionic conductivity. The ionic conductivity behaviour of the sample was shown to follow structural changes and was likely related to the different boron species which act as lithium sites. This conclusion was drawn from the fact that the number of non-bridging oxygens increases proportionally to the lithium to boron ratio when $R \geq 0.5$. The study also identified two lithium species within the glass.

From Amorphous to Ordered: Structural Transformation of Pd Nanoclusters in 1-Pentyne Hydrogenation Reactions

K.-J. Hu, P. R. Ellis, C. M. Brown, P. T. Bishop and R. E. Palmer, *J. Catal.*, 2021, **397**, 58

This study aimed to investigate the structural transformation of monodispersed palladium nanoclusters using a vapour-phase 1-pentyne hydrogenation reaction. Aberration-corrected STEM was used to examine the structural transformation of the palladium nanoclusters at the atomic level. A distinctive structural transformation was observed, and after the full 1-pentyne hydrogenation reaction, both $Pd_{2057\pm45}$ and $Pd_{923\pm20}$ amorphous clusters transformed into highly symmetrical structures. This work provides a new insight into the long-term stability of commercial heterogenous catalysts.

Stepwise Collapse of a Giant Pore Metal–Organic Framework

A. F. Sapnik, D. N. Johnstone, S. M. Collins, G. Divitini, A. M. Bumstead, C. W. Ashling, P. A. Chater, D. S. Keeble, T. Johnson, D. A. Keen and T. D. Bennett, *Dalton Trans.*, 2021, **50**, (14), 5011

The properties of MOFs can be tailored through defect engineering. In this study, defects were encompassed *via* ball milling to methodically alter the porosity of the giant pore MOF, MIL-100 (Fe). Milling was revealed to generate additional coordinatively unsaturated metal sites through the breaking of metal-linker bonds. This ultimately led to amorphisation. However, even in the amorphised material, the hierarchical local structure was partially retained, as observed by pair distribution function analysis. The MIL-100 (Fe) framework was stabilised against collapse when solvents were used, which led to a significant retention of porosity over the non-stabilised material.

Enantio-Complementary Continuous-Flow Synthesis of 2-Aminobutane Using Covalently Immobilized Transaminases

C. M. Heckmann, B. Dominguez and F. Paradisi, *ACS Sustain. Chem. Eng.*, 2021, **9**, (11), 4122

This work studied the synthesis of 2-aminobutane, one of the smallest chiral amines, using transaminases. Two transaminase candidates were identified after screening. These were a precommercial (*R*)-selective transaminase from Johnson Matthey (*RTA-X43) and an (*S*)-selective transaminase from *Halomonas elongata* (HEwT). The enantioselectivity of HEwT was enhanced from 45% to 99.5% enantiomeric excess. The candidates were covalently immobilised, leading to the synthesis of both enantiomers of 2-aminobutane on a multigram scale. The *E*-factors, including immobilisation and waste generated through enzyme expression, were 48 for the synthesis of (*S*)-2-aminobutane and 55 for the synthesis of (*R*)-2-aminobutane. The atom economy of the process was 56%.

Multiscale Modeling and Analysis of Pressure Drop Contributions in Catalytic Filters

M. Leskovjan, J. Němec, M. Plachá, P. Kočí, M. Isoz, M. Svoboda, V. Novák, E. Price and D. Thompsett, *Ind. Eng. Chem. Res.*, 2021, **60**, (18), 6512

A multiscale modelling methodology was used for the prediction of filter pressure loss, dependent on the microscopic structure of the wall (i.e. catalytic coating) and the monolith channel geometry. The process was based on a mixture of a 1D+1D model of the filter channels and a 3D pore-scale model of flow through the wall, reconstructed from XRT. Several experiments were performed on SiC filter and cordierite samples with varying catalyst distributions and pore sizes. To determine individual pressure drop contributions (inlet and outlet, wall and channel), investigations were completed at different filter lengths and gas flow rates. The predicted pressure drop agreed well with the experiments and displayed the strong impact of the coating location.

Use of 3D-Printed Mixers in Laboratory Reactor Design for Modelling of Heterogeneous Catalytic Converters

M. Walander, A. Nygren, J. Sjöblom, E. Johansson, D. Creaser, J. Edvardsson, S. Tamm and B. Lundberg, *Chem. Eng. Process. Process Intensif.*, 2021, **164**, 108325

This study presents a new method for identifying radial concentration maldistribution in synthetic catalyst activity test (SCAT) benches. A static mixer of the authors' design was 3D printed and inserted upstream the test sample (**Figure 1**). The mixer resolved a radial concentration maldistribution. A

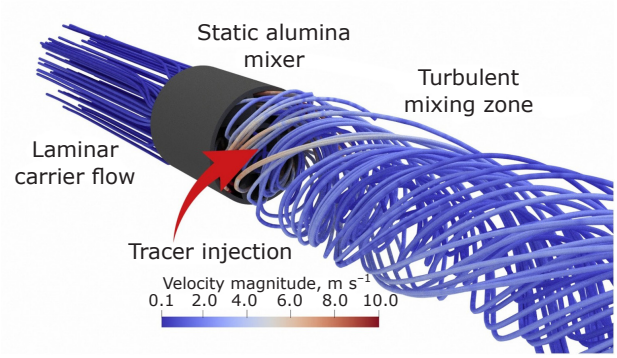

Fig. 1. Reprinted from M. Walander *et al*., *Chem. Eng. Process. Process Intensif*., 2021, **164**, 108325, Copyright (2021), with permission from Elsevier

3D CFD model and classical Aris-Taylor calculations were used to compare the axial dispersion of a remixed SCAT bench and an injection-based SCAT bench. In terms of pulse broadening and time delay, the premixed design was inferior to the injection-based design with the use of a static mixer.

Application of Hydrodynamic Lubrication in Discrete Element Method (DEM) Simulations of Wet Bead Milling Chambers

R. Cabiscol, T. Jansen, M. Marigo and C. Ness, *Powder Technol.*, 2021, **384**, 542

The authors present a DEM simulation for a laboratory scale mill, which includes pairwise hydrodynamic lubrication in addition to frictional forces. A systematic model calibration against the laboratory mill at variable operation conditions (such as feed viscosities and rotation speeds) was exhibited. Further investigation into the local distribution of collisions along the mill chamber and the differences in energy dissipation modes showed that the majority of energy dissipation was attributed to interparticle forces acting tangentially. Conversely, highly energetic collisions that are reliant on interbed mobility and free flows were relatively unimportant.

Transport Studies of $NaPF_6$ Carbonate Solvents-Based Sodium Ion Electrolytes

D. Morales, L. G. Chagas, D. Paterno, S. Greenbaum, S. Passerini and S. Suarez, *Electrochim. Acta*, 2021, **377**, 138062

The bulk and local transport properties of 1 M $NaPF_6$ in binary and ternary solvents, along with their 2 wt% FEC modulated versions, was investigated. ^{1}H, ^{19}F and ^{23}Na NMR spin-lattice relaxation time (T_1) was determined along with chemical shift,

linewidth, viscosity, density and ionic conductivity. The Walden products of ionic conductivity and viscosity demonstrated a dependence on temperature, and the prevalence of lower Walden products suggested less salt dissociation in the 5EC:3PC:2DEC and 5EC:3PC:2DEC + 2 wt% electrolytes. The incorporation of FEC allowed for greater local dynamics for the individual solvents in the less polar electrolyte. However, it seemed to hinder that of the ions.

Elucidation of Copper Environment in a Cu–Cr–Fe Oxide Catalyst Through *in situ* High-Resolution XANES Investigation

T. Lais, L. Lukashuk, L. van de Water, T. I. Hyde, M. Aramini and G. Sankar, *Phys. Chem. Chem. Phys.*, 2021, **23**, (10), 5888

To determine the local site symmetry of copper ions during the thermal treatment of a Cu-Cr-Fe oxide catalyst, this study used a copper K-edge high resolution XANES. To determine the local environment of Cu^{2+} ions, spectral features of the copper K-edge high resolution XANES, such as the correlation between its position and the area under the pre-edge peak, were exploited. Results from the study highlighted that the Cu^{2+} ions in the Cu-Cr-Fe oxide system were present in a distorted octahedral environment. On the other hand, the Cu^{2+} ions were not present in a reduced oxidation state, in a tetrahedral or square planar geometry or a mixture of these sites.